Inorg. Chem. **2006**, *45*, 8264–8272

Syntheses, Structures, Physical Properties, and Theoretical Studies of CeM_xOS (M = Cu, Ag; $x \approx 0.8$) and CeAgOS

George H. Chan,[†] Bin Deng,[#] Mariana Bertoni,[†,#] John R. Ireland,[#] Mark C. Hersam,[#] Thomas O. Mason,[#] Richard P. Van Duyne,[†] and James A. Ibers*,[†]

Department of Chemistry, Northwestern University, 2145 Sheridan Road, Evanston, Illinois 60208-3113, and Department of Materials Science and Engineering, Northwestern University, 2220 Campus Drive, Cook Hall, Evanston, Illinois 60208-3108

Received June 10, 2006

Black single crystals of the two nonstoichiometric cerium coinage-metal oxysulfide compounds $CeCu_xOS$ and $CeAg_xOS$ ($x \approx 0.8$) have been prepared by the reactions of Ce_2S_3 and CuO or Ag_2O at 1223 or 1173 K, respectively. A black powder sample of CeAgOS has been prepared by the stoichiometric reaction of Ce_2S_3, CeO_2, Ag_2S, and Ag at 1073 K. These isostructural materials crystallize in the ZrSiCuAs structure type with two formula units in the tetragonal space group *P*4/*nmm*. Refined crystal structure results and chemical analyses provide evidence that the previously known anomalously small unit-cell volume of LnCuOS for Ln = Ce (Ln = rare-earth metal) is the result of Cu vacancies and the concomitant presence of both Ce^{3+} and Ce^{4+}. Both $CeCu_{0.8}OS$ and CeAgOS are paramagnetic with μ_{eff} values of 2.13(6) and 2.10(1) μ_B, respectively. $CeCu_{0.8}OS$ is a *p*-type semiconductor with a thermal activation energy $E_a = 0.22$ eV, $\sigma_{electrical} = 9.8(1)\ 10^{-3}$ S/cm at 298 K, and an optical band gap $E_g < 0.73$ eV. CeAgOS has conductivity $\sigma_{conductivity} = 0.16(4)$ S/cm and an optical band gap $E_g = 0.71$ eV at 298 K. Theoretical calculations with an on-site Coulomb repulsion parameter indicate that the Ce 4f states are fully spin-polarized and are not localized in CeCuOS, $CeCu_{0.75}OS$, or CeAgOS. Calculated band gaps for $CeCu_{0.75}OS$ and CeAgOS are 0.6 and 0.8 eV, respectively.

Introduction

The two-dimensional layered nature of quaternary metal oxychalcogenides is a result of "hard" cations preferring to coordinate to smaller oxide anions and more polarizable "soft" cations preferring to coordinate to larger chalcogenide anions. This allows for the simple design by cation substitution of new compounds with interesting transport and optical properties. For example, the structure of $CeMn_{0.5}OSe$ is built from $(Ce_2O_2)^{2+}$ and $(MnSe_2)^{2-}$ layers. This dark-orange compound has a band gap of 2.01 eV in the [100] direction.[1] In contrast, the structure of $La_2CdO_2Se_2$ is built from $(La_2O_2)^{2+}$ and $(CdSe_2)^{2-}$ layers; its band gap is 3.3 eV.[2]

Rare-earth coinage-metal oxychalogenides, LnMOQ (Ln = rare-earth; M = Cu, Ag; Q = S, Se, Te) are a class of layered materials that consist of alternating $(Ln_2O_2)^{2+}$ oxide layers and $(M_2Q_2)^{2-}$ chalcogenide layers stacked perpendicular to the *c* axis in a tetragonal cell.[3,4] The two-dimensional nature of these compounds, the $(M_2Q_2)^{2-}$ layer in particular, is the origin of the interesting transport and optical properties. For instance, LaAgOS,[4−7] the only reported silver compound of this type, is an *n*-type fast-ion conductor with $\sigma_{ionic} = 10^{-3}$ to 10^{-1} S/cm between 298 and 523 K, whereas the LnCuOS (Ln = La −Nd) compounds are direct band gap *p*-type semiconductors with high electrical conductivities.[8,9] Moreover, LaCuOS is optically transparent in the visible

* Author to whom correspondence should be addressed. Email: ibers@chem.northwestern.edu.
[†] Department of Chemistry.
[#] Department of Material Science and Engineering.

(1) Ijjaali, I.; Mitchell, K.; Haynes, C. L.; McFarland, A. D.; Van Duyne, R. P.; Ibers, J. A. *J. Solid State Chem.* **2003**, *176*, 170−174.
(2) Hiramatsu, H.; Ueda, K.; Kamiya, T.; Ohta, H.; Hirano, M.; Hosono, H. *J. Phys. Chem. B* **2004**, *108*, 17344−17351.
(3) Palazzi, M. *C. R. Acad. Sci., Sér. 2* **1981**, *292*, 789−791.
(4) Palazzi, M.; Carcaly, C.; Flahaut, J. *J. Solid State Chem.* **1980**, *35*, 150−155.
(5) Palazzi, M.; Jaulmes, S. *Acta Crystallogr. Sect. B: Struct. Sci.* **1981**, *37*, 1337−1339.
(6) Schiffmacher, G.; Palazzi, M. *Mater. Res. Bull.* **1981**, *16*, 1401−1405.
(7) Wilmer, D.; Jorgensen, J. D.; Wuensch, B. J. *Solid State Ionics* **2000**, *136*−*137*, 961−966.
(8) Ueda, K.; Takafuji, K.; Hiramatsu, H.; Ohta, H.; Kamiya, T.; Hirano, M.; Hosono, H. *Chem. Mater.* **2003**, *15*, 3692−3695.
(9) Ueda, K.; Hiramatsu, H.; Hirano, M.; Kamiya, T.; Hosono, H. *Thin Solid Films* **2006**, *496*, 8−15.

10.1021/ic061041k CCC: $33.50
Published on Web 09/07/2006

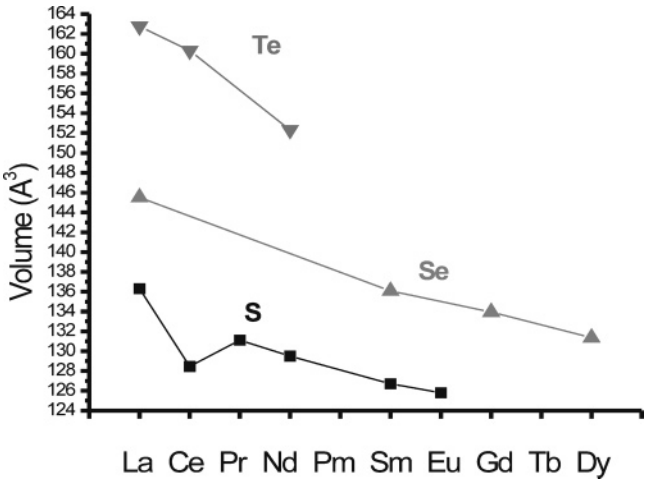

Figure 1. Unit cell volumes of LnCuOQ compounds as a function of Ln. The Q = S data are from refs 3 and 11; the Q = Se data are from refs 11 and 40; the Q = Te data are from ref 38.

region and has been classified as a *p*-type transparent conducting oxide semiconductor. Photoluminscence measurements (Ln = La, Pr, and Nd) indicate that the fundamental optical properties and excitons are confined in the $(Cu_2S_2)^{2-}$ layer.[8] An electronic structure study of LaCuOQ (Q = S, Se, Te) carried out by the FLAPW method using LDA+U suggests that the S and Se compounds should be direct-gap semiconductors, whereas the Te compound should be an indirect-gap semiconductor.[10]

Figure 1 displays the unit cell volumes of the known LnCuOQ structures as a function of Ln and Q. Note that the Q = Se and Te compounds obey the expected lanthanide contraction. However, in the LnCuOS series the unit-cell volume of CeCuOS does not follow the lanthanide contraction but is anomalously small, as deduced from studies of powders.[11,12] This has been ascribed to nonstoichiometry[11] or to short Ce−S distances.[12] Moreover, CeCuOS shows *p*-type degenerate semiconducting behavior at low temperatures and an unusually high electrical conductivity at room temperature.[8] In addition, CeCuOS is black, unlike its rare-earth analogues.

It is clear that the composition, structure, and physical properties of CeCuOS need further investigation. Here we report the syntheses of the first single crystals, as opposed to powders, of the compound we characterize as $CeCu_xOS$ ($x \approx 0.8$). In addition to its crystal structure, we report chemical analyses, magnetic susceptibility, electrical conductivity, optical properties, and an electronic structure calculation of this compound. We also report the synthesis and structural characterization of single crystals of the new compound $CeAg_xOS$ ($x \approx 0.8$). In addition, a powder sample of CeAgOS has been synthesized and characterized. We present some physical properties and electronic structure calculations of CeAgOS.

(10) Ueda, K.; Hosono, H.; Hamada, N. *J. Phys.: Condens. Matter* **2004**, *16*, 5179−5186.
(11) Charkin, D. O.; Akopyan, A. V.; Dolgikh, V. A. *Russ. J. Inorg. Chem. (Transl. of Zh. Neorg. Khim.)* **1999**, *44*, 833−837.
(12) Ueda, K.; Takafuji, K.; Hosono, H. *J. Solid State Chem.* **2003**, *170*, 182−187.

Table 1. X-ray Crystallographic Data for CeMOS[a]

formula	$CeCu_{0.809}OS$	$CeCu_{0.762}OS$	$CeAg_{0.777}OS$	$CeAg_{0.763}OS$
fw	239.59	236.60	272.00	270.49
a (Å)	3.9142(3)	3.9072(3)	3.9256(3)	3.9230(3)
c (Å)	8.2980(10)	8.2834(10)	8.9943(9)	9.0130(8)
V (Å^3)	127.13(2)	126.46(2)	138.61(2)	138.71(2)
T (K)	153(2)	298(2)	153(2)	298(2)
ρ_{calc} (g cm^{-3})	6.259	6.214	6.517	6.476
μ (cm^{-1})	249.4	246.9	221.7	220.6
R1[b]	0.0190	0.0174	0.0137	0.0137
wR2[c]	0.0539	0.0390	0.0382	0.0430
q	0.03	0.02	0.025	0.025

[a] For all structures $Z = 2$, space group = $P4/nmm$ and $\lambda = 0.71073$ Å. [b] $R1 = \sum||F_o| - |F_c||/|F_o|$ for $F_o^2 > 2\sigma(F_o^2)$. [c] $wR2 = \{\sum[w(F_o^2 - F_c^2)^2]/\sum wF_o^4\}^{1/2}$ for all data. $w^{-1} = \sigma^2(F_o^2) + (qP)^2$, where $P = (\max(F_o^2,0))$.

Experimental Section

Syntheses. Single crystals of the compounds CeM_xOS (M = Cu, Ag; $x \approx 0.8$) synthesized here will be designated generically as $CeCu_{0.8}OS$ or $CeAg_{0.8}OS$. Those of $CeCu_{0.8}OS$ were obtained from the reaction of 0.5 mmol of Ce_2S_3 (Alfa Aesar, 99.9%) with 0.6 mmol of CuO (Alfa, 99.99%); 150 mg of KCl (Aldrich, 99.99%) was added as flux to promote crystallization. The carbon-coated fused-silica reaction tube was sealed at 10^{-4} Torr and then placed into a computer-controlled furnace where it was heated to 1223 K in 24 h, kept at 1223 K for 96 h, and then cooled to 298 K at 2 K/h. The product was washed with deionized water and dried with acetone. It consisted of a mixture of black square plates of $CeCu_{0.8}OS$ and red plates of $CeCuS_2$. The yield of $CeCu_{0.8}OS$ was approximately 50% based on CuO.

Single crystals of $CeAg_{0.8}OS$ were obtained from the reaction of 0.5 mmol of Ce_2S_3 (Alfa Aesar, 99.9%) with 0.6 mmol of Ag_2O (Alfa Products, 99%); 150 mg of KBr (Aldrich, 99.99%) flux was added. The carbon-coated fused-silica reaction tube was sealed at 10^{-4} Torr and then placed into a computer-controlled furnace where it was heated to 773 K in 24 h, kept at 773 K for 48 h, heated to 1173 K in 10 h, held at 1173 K for 96 h, and cooled to 573 K at 3 K/h, and then the furnace was turned off. The product consisted of a few black needles of $CeAg_{0.8}OS$.

A powder phase of CeAgOS was obtained in a rational manner from the stoichiometric reaction of Ce_2S_3 (Alfa Aesar, 99.9%), Ag_2S (Alfa Aesar, 99%), CeO_2 (Aldrich, 99.999%), and Ag (Aldrich, 99.99+%) in a molar ratio of 1:1:2:2. The carbon-coated reaction tube was sealed at 10^{-4} Torr and then placed into a computer-controlled furnace where it was heated to 1073 K at 25 K/min and held there for 3 days, and then the furnace was quickly cooled to 298 K at 100 K/min. The product was ground, reloaded into a new carbon-coated tube, and the same heating procedure was applied. A calibrated X-ray powder diffraction pattern of the product was obtained with Cu Kα radiation at 298 K on a Rigaku powder diffractometer. Comparison of this experimental X-ray powder diffraction pattern with the theoretical pattern simulated from the single-crystal X-ray data collected at 298 K provided no indication of the presence of Ag metal or other impurities. The refined unit cell constants from the powder are $a = b = 3.9550(1)$ Å, $c = 9.0734(1)$ Å. The unit-cell volume of 141.92 Å^3 is larger than those of $CeAg_{0.8}OS$ determined at 153 and 298 K (Table 1). We therefore refer to this phase as CeAgOS.

EDX Analyses. Energy-dispersive X-ray (EDX) analyses were carried out with the use of an Hitachi S-3500 SEM. Data were collected with an accelerating voltage of 20 keV, a working distance of 15 mm, and a collection time of 60 s. Selected single crystals of $CeCu_{0.8}OS$ and $CeAg_{0.8}OS$ showed the presence of Ce, Ag or Cu, S, and O.

Inductively Coupled Plasma (ICP) Measurement. A VISTA-MPX CCD Simultaneous Varian ICP-OES was used to measure the molar ratio of Cu/Ce for $CeCu_{0.8}OS$. Single crystals (1.5 mg) of $CeCu_{0.8}OS$ were dissolved in 3 mL of HNO_3, and the solution was adjusted to a volume of 10 mL with MQ water. The Cu/Ce ratio was determined to be 0.78(1). Unfortunately, chemical analyses of single crystals of $CeAg_{0.8}OS$ could not be performed, owing to the very low yield of this compound. Because of the stoichiometric loading, no ICP measurements were made on CeAgOS powder.

Crystal Structure Determinations. Single-crystal X-ray diffraction data were obtained for both $CeCu_{0.8}OS$ and $CeAg_{0.8}OS$ at 153 and 298 K. Different crystals from different preparations were used at each temperature. The four data sets were collected on a Bruker Smart 1000 CCD diffractometer[13] with the use of monochromatized Mo Kα radiation ($\lambda = 0.71073$ Å). The crystal-to-detector distance was 5.023 cm. Crystal decay was monitored by collecting 50 initial frames at the end of the data collection. The diffracted intensities were generated by a scan of 0.3° in ω in groups of 606 frames for each of the φ settings 0°, 90°, 180°, and 270°. The exposure times were 10 (153 K) and 20 s/frame (298 K) for $CeCu_{0.8}OS$ and 15 (153 K) and 20 s/frame (298 K) for $CeAg_{0.8}OS$. Intensity data were collected with the program SMART.[13] Cell refinement and data reduction were carried out with the program SAINT,[13] and numerical face-indexed absorption corrections were made with the use of the program XPREP.[14] Finally, the program SADABS[14] was employed to make incident beam and decay corrections.

These materials crystallize with two formula units in the tetragonal space group *P*4/*nmm*. The crystal structures were solved with the direct-methods program SHELXS[14] and refined with the full-matrix least-squares program SHELXL.[14] The program STRUCTURE TIDY[15] was used to standardize the positional parameters.

The refinements of the Cu data sets improved considerably when it was assumed that the crystals were deficient in Cu. For example, refinement of the 153 K data set on the assumption of full occupancy led to values of the agreement indices R1 and wR2 of 0.041 and 0.115, respectively, and to an unsatisfactory suggested weighting scheme. Refinement with the occupancy of the Cu site as an additional variable led to the agreement indices 0.019 and 0.0539, respectively, and to a satisfactory suggested weighting scheme. The resultant formula is $CuCu_{0.809(4)}OS$.

The refinements of the Ag data sets also improved considerably when Ag deficiencies were assumed. For example, for the 153 K data, the values of R1 and wR2 decreased from 0.043 and 0.111 to 0.026 and 0.090, respectively. However, some of the mean-square atomic displacements of the Ag atom were as large as 0.081 Å^2. With the use of JANA2000,[16] a refinement of a model that included anharmonic displacements brought about a minimal improvement. Consequently, the Ag atom at 3/4, 1/4, 0 (Wyckoff position 2a) was split into two and the half atoms were placed at the $1/2 + x$, $1/2 - x$, 0 positions (Wyckoff position 8g) with x as an additional variable. This refinement converged to values of R1 and wR2 of 0.0137 and 0.0382, respectively, and to a separation of the Ag pair of 0.417(3) Å. The resultant mean-square atomic displacements of the Ag atom were now all less than 0.025 Å^2. The resultant formula is $CeAg_{0.777(4)}OS$. For the Ag data at 298 K treated in a similar manner, the refinement converged to values of R1 and wR2 of 0.0137 and 0.0430, respectively, and to a separation of the Ag pair of 0.34(2) Å. The resultant mean-square atomic displacements of the Ag atom are lower but remain as high as 0.0798 Å^2. The resultant formula is $CeAg_{0.763(3)}OS$. Additional experimental details are shown in Table 1 and in the Supporting Information.

Magnetic Susceptibility Measurements. DC magnetic susceptibility measurements on ground single crystals of $CeCu_{0.8}OS$ and a powder sample of CeAgOS were carried out with the use of a Quantum Design MPMS5 SQUID magnetometer. The samples, 34.9 mg of $CeCu_{0.8}OS$ and 34.8 mg of CeAgOS, were loaded into gelatin capsules. In the temperature range between 5 and 350 K, both zero-field cooled (ZFC) and field cooled (FC) measurements were processed with a 500 G applied field. All data were corrected for electron core diamagnetism.[17]

Diffuse Reflectance Measurements. Diffuse reflectance spectra over the range 400 (3.1 eV) to 2600 nm (0.48 eV) at 298 K of a powder sample of CeAgOS were obtained with a Varian Cary 5000 UV/vis/NIR double-beam spectrometer equipped with a diffuse reflectance accessory. The absorption (α/S) data were calculated from the reflectance data with the use of the Kubelka−Munk function $\alpha/S = (1 - R)^2/2R$, where R is the reflectance at a given energy, α is the absorption coefficient, and S is the scattering coefficient.[18]

Transport Measurements. The composition of two black plates of $CeCu_{0.8}OS$ (0.5 mm × 0.5 mm × 0.05 mm) was confirmed with EDX measurements. The electrical conductivity and Hall measurements of these two single crystals were obtained with the use of the computer-controlled, four- and five-probe technique, respectively.[19] Electrical contacts consisted of fine gold wire attached to the crystals with gold paste. To improve contact performance, the samples were placed under vacuum for at least 24 h to allow the gold paste to cure completely. Excitation currents were kept as low as possible, typically below 1 mA, to minimize any nonohmnic voltage response and thermoelectric effects at the contact−sample interface, and the currents were rapidly switched to minimize any thermoelectric effects. Hall measurements were made with a magnetic flux density of 0.74 T. Measurements of the sample cross-sectional area and voltage probe separation were made with a calibrated binocular microscope.

Conductivity measurements on CeAgOS powder were performed by means of the powder−solution−composite (PSC) technique.[20] In this technique, the bulk conductivity of a ceramic powder is obtained by measuring the impedance spectra of "composite" slurries of the powder with electrolytic solutions. In the present instance, the electrolytes were aqueous solutions of NaCl that ranged in concentration from 0.002 ($2.6\ 10^{-4}$ S/cm) to 4.8 M (0.25 S/cm). Each of these solutions was mixed with 0.07 g of CeAgOS powder to form a slurry, which was then placed into the measuring device and allowed to settle. The measuring apparatus consisted of a polyethylene tube (4.6 mm i.d. × 22.8 mm) and two stainless steel end plugs. The composite was carefully pressed to a volume fraction of powder of approximately 0.3 (at an inner-electrode spacing of 2 mm). An HP 4192A impedance response analyzer was employed with Labview personal computer software for data collection.

(13) *SMART Version 5.054 Data Collection* and *SAINT-Plus Version 6.45a Data Processing Software for the SMART System*; Bruker Analytical X-ray Instruments, Inc.: Madison, WI, 2003.
(14) Sheldrick, G. M. *SHELXTL Version 6.14*; Bruker Analytical X-ray Instruments, Inc.: Madison, WI, 2003.
(15) Gelato, L. M.; Parthé, E. *J. Appl. Crystallogr.* **1987**, *20*, 139−143.
(16) Petříček, V.; Dušek, M. *Jana2000*; Institute of Physics, Academy of Science of the Czech Republic: Prague, 2000.
(17) Mulay, L. N.; Boudreaux, E. A., Eds. *Theory and Applications of Molecular Diamagnetism*; Wiley-Interscience: New York, 1976.
(18) Tandon, S. P.; Gupta, J. P. *Phys. Status Solidi A* **1970**, *37*, 43−45.
(19) Lyding, J. W.; Marcy, H. O.; Marks, T. J.; Kannewurf, C. R. *IEEE Trans. Instrum. Meas.* **1988**, *37*, 76−80.
(20) Ingram, B. J.; Mason, T. O. *J. Electrochem. Soc.* **2003**, *150*, E396-E402.

Alligator clips at the end of coaxial cables were used to make electrical connections to the stainless steel plugs. The excitation voltage was 1 V, and the scans were performed from 10 MHz to 1 Hz, with data collected at 10 steps per frequency decade.

Electronic Structure. Calculations were performed with the Wien2k code in the full-potential plane wave (FLAPW) method.[21] The exchange−correlation potentials were treated in the generalized gradient approximation (GGA) within density function theory.[22] A Hubbard parameter *U* of 2.0 eV was used to treat Coulomb on-site interactions for Ce in the GGA+U scheme.[22,23] For the calculations of CeCuOS,[12] CeAgOS, and $CeCu_{0.75}OS$, the muffin-tin radii were chosen as 2.5 Bohr for Ce, 2.5 Bohr for Ag, 2.35 Bohr for Cu, 2.2 Bohr for S, and 1.9 Bohr for O. For the calculation of LaAgOS,[5] the muffin-tin radii were chosen to be 2.5 Bohr for La, 2.5 Bohr for Ag, 2.2 Bohr for S, and 1.9 Bohr for O.

To model the Cu atom deficiencies in $CeCu_{0.8}OS$, one Cu atom was substituted by a vacancy in a 2 × 1 supercell of CeCuOS, which resulted in a cell containing three unique Ce, S, and O atoms and two unique Cu atoms. The resultant chemical formula is $CeCu_{0.75}OS$. We therefore approximate the electronic structure of $CeCu_{0.8}OS$ with that of $CeCu_{0.75}OS$. In addition, we have calculated the electronic structure of CeCuOS to compare with that of $CeCu_{0.75}OS$. Unfortunately, similar calculations for $CeAg_{0.75}OS$ did not converge, owing to charge fluctuation between the interstitial regions and the muffin-tin radii. Hence, we have calculated the electronic structure of CeAgOS, which represents the powder sample. To do this, the structural results for $CeAg_{0.8}OS$ were used but with full occupancy of the Ag site. The plane-wave expansion cutoff for wave functions (RK_{max}) was set at 7, and those for the densities and potentials (G_{max}) were set at 16 $Bohr^{-1}$, respectively. In the Brillouin zone, 200 *k* points were used for CeCuOS, CeAgOS, and LaAgOS, whereas 100 *k* points were used for $CeCu_{0.75}OS$. The calculations were iterated self-consistently until the total electron density did not change by more than 0.0001 e^-.

Results and Discussion

Syntheses. Single crystals of $CeCu_{0.8}OS$ were synthesized in about 50% yield by the reaction of Ce_2S_3 with CuO in a KCl flux at 1223 K. Efforts to synthesize a powder phase of $CeCu_xOS$ or single crystals of stoichiometric CeCuOS starting from various reactants and different heating profiles were unsuccessful. For example, in an attempt to make a powder phase of $CeCu_{0.8}OS$, a mixture of Ce_2S_3, CuO, CeO_2, and Cu (1:1:1:1.8 molar ratio) was heated at 1073 K for 72 h. X-ray powder diffraction analyses of the product indicated the presence of Ce_2O_2S and Cu_2S but not of $CeCu_{0.8}OS$. Additional attempts were made with the use of CeO_2, Cu_2S, Ce_2S_3, and Cu, but these reactions yielded neither CeCuOS nor $CeCu_xOS$. Reactions of Ce_2S_3 and CuO in varying ratios (e.g., 1:3; 2:1.5; 2:3.5; 1:4) were heated with the addition of KCl or KI (to aid in crystal growth) at 1223 K for 96 h. However, no single crystals of $CeCu_xOS$ were obtained. These products were washed with deionized water, dried with acetone, ground with a mortar and pestle, and then analyzed by means of powder X-ray diffraction methods. Only binary and ternary Ce and Cu compounds were present, e.g., $CeCuS_2$.

The synthetic routes used here differ from those used previously to prepare powders. In one such study[11] two different routes were used to prepare samples. In one, Ce, S, and CuO (1:1:1 molar ratio) were exposed to salt melts of NaCl:KCl in a 1:1 molar ratio at 1193 K for 10 days; in the second, pellets containing mixtures of Ce, CeO_2, Cu, and S (1:1:2:2 molar ratio) were exposed to salt melts of NaCl/KCl in a 1:1 molar ratio between 573 and 673 K for 3 days and then annealed between 1153 and 1173 K for 10 days. These syntheses resulted in a series of samples described as $CeCu_xOS$ for varying *x*. No chemical analyses were performed. In a second study[12] a powder phase described as CeCuOS was prepared by heating powders of CeO_2 and Cu_2S (2:1) in an atmosphere of dilute H_2S gas at 1073 K for 2 h and then subsequently annealing the sample at 1073 K for 6 h. ICP chemical analysis and X-ray powder diffraction analyses were taken as evidence that stoichiometric CeCuOS had been obtained, but it was noted that the possibility of a Cu deficiency remained.

A few single crystals of $CeAg_{0.8}OS$ were synthesized in the reaction of Ce_2S_3 with Ag_2O in a KBr flux at 1173 K. Extensive efforts to increase the yield by changing the heating profile or the molar ratios of the starting materials or the flux or the starting materials themselves were unsuccessful. A powder phase of CeAgOS was obtained readily in the stoichiometric reaction of Ce_2S_3, Ag_2S, CeO_2, and Ag at 1073 K. The difficulty of obtaining single crystals but the ease of obtaining a powder parallels the experience with the La analogue.[7] For several reasons, we believe that the powder phase is stoichiometric CeAgOS, rather than $CeAg_{0.8}OS$, as were the single crystals. If the powder phase were the latter and if the reaction were

$$Ce_2S_3 + Ag_2S + 2CeO_2 + 2Ag \rightarrow 4CeAg_{0.75}OS + Ag$$

then the resultant material would have contained approximately 9 wt % of Ag metal. There is no evidence for Ag or any other impurity in the X-ray powder pattern of the

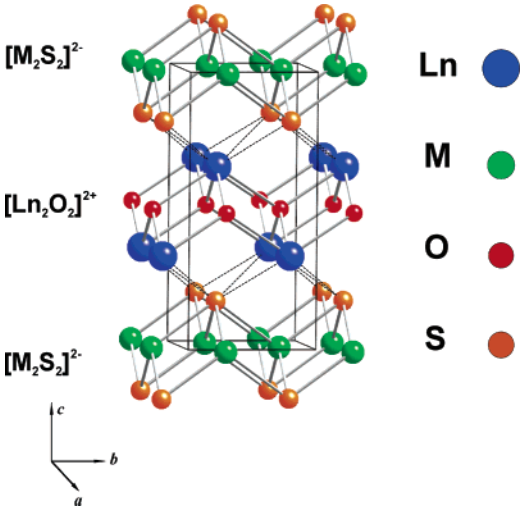

Figure 2. Unit cell of LnMOS (Ln = rare-earth element).

(21) Blaha, P.; Schwarz, K.; Madsen, G. K.; Kvasnicka, D.; Luitz, J. *WIEN2k. An Augmented Plane Wave + Local Orbitals Program for Calculating Crystal Properties*; Karlheinz Schwarz, Technische Universität Wien Austria: Vienna, 2001.
(22) Perdew, J. P.; Burke, K.; Ernzerhof, M. *Phys. Rev. Lett.* **1996**, *77*, 3865−3868.
(23) Czyzyk, M. T.; Sawatzky, G. A. *Phys. Rev. B* **1994**, *49*, 14211−14228.

Table 2. Selected Bond Distances (Å) for CeMOS

distance	$CeCu_{0.809}OS^a$	$CeCu_{0.762}OS^b$	$CeAg_{0.777}OS^a$	$CeAg_{0.763}OS^b$
Ce−O × 4	2.3331(3)	2.3342(2)	2.3404(2)	2.3399(2)
Ce−S × 4	3.1374(10)	3.1245(8)	3.1206(7)	3.1210(8)
Cu−S × 4	2.4072(11)	2.4064(9)		
Ag−S × 2			2.520(2)	2.546(6)
M−M × 4	2.7678(2)	2.7628(2)	2.7758(1)	2.7740(2)

[a] 153 K. [b] 298 K.

material, although the first nonoverlapping Ag peak would occur at 64.5° 2θ. Moreover, the above reaction implies that 25% of the Ce^{3+} cations have been oxidized to Ce^{4+} with concomitant reduction of Ag^+ to Ag. Although it is impossible to extrapolate to the actual reaction conditions, it is worth noting that in aqueous systems Ce^{4+} is a powerful oxidant that readily takes Ag to Ag^+. Finally, the presence of Ag metal would markedly affect the conductivity of the sample.

Crystal Structure. The refined model for the structure of $CeAg_{0.8}OS$, which involves Ag disorder and harmonic vibrations, affords the best fit to the electron density. The Bragg X-ray experiment affords only the approximate electron density and not its interpretation, which is in the eye of the beholder. Thus, whether the Ag cations are indeed disordered over two sites in the structure of $CeAg_{0.8}OS$ or whether this is an artifact of the fitting process is not clear. With that caveat, we consider the compounds $CeCu_{0.8}OS$ and $CeAg_{0.8}OS$ to be isostructural and of the ZrSiCuAs[24] structure type. The crystal structure of the isostructural LnMOS materials is illustrated in Figure 2, and selected bond distances are given in Table 2.

The compounds $CeCu_{0.8}OS$ and $CeAg_{0.8}OS$ are built from alternating $[Ce_2O_2]$ fluorite-like and $[M_2S_2]$ (M = Cu, Ag) antifluorite-like layers stacked perpendicular to the *c* axis. Each Ce atom, with site symmetry 4*mm*, is coordinated to four O atoms in one base and four S atoms in the other to form a distorted square antiprism. The Ce−O bond distances (Table 2) are comparable to that of 2.3533(5) Å in the structure of $CeMn_{0.5}OSe$;[1] the Ce−S bond is comparable to that of 3.10(1) Å in $BiCeOS_2$.[25] The Cu atom (site symmetry 4*m*2) is coordinated to four S atoms in a nearly regular tetrahedron. The Cu−S distance is comparable to those in $La_5Cu_6O_4S_7$[26] (2.353(1)−2.477(1) Å) and in $La_3CuO_2S_3$[27] (2.316(2)−2.390(1) Å); the Cu−Cu distance is comparable to those in $La_5Cu_6O_4S_7$[26] (2.5865(7)−2.965(1) Å). In the disordered model for the $CeAg_{0.8}OS$ structure, the Ag atom has site symmetry 2 and is about 0.2 Å from the 4*m*2 site occupied by the Cu atom in $CeCu_{0.8}OS$. The resultant distances involving Ag (Table 2) may therefore not be representative. Nevertheless, the Ag−S distance is comparable to those in $AgCd_2GaS_4$[28] (2.541(3)−2.558(3) Å) and to that of 2.673(6) Å in LaAgOS.[5,7] The Ag−Ag distance may be compared with those in KAg_5S_3[29] (2.948(2)−3.001(2) Å) and that in LaAgOS[5,7] (2.886 Å).

Table 3. Soft Bond Valence Sums for LnCuOS

compound	Ln	Cu	ref
PrCuOS	3.06	0.89	12
PrCuOS	3.08	0.84	11
NdCuOS	3.09	0.89	12
LaCuOS	3.13	0.81	3
LaCuOS	3.15	0.84	12
CeCuOS	3.23	0.85	12
$CeCu_{0.809}OS$	3.25	0.88	this work
$CeCu_{0.762}OS$	3.28	0.88	this work

Bond Valence Calculations. In $CeCu_{0.8}OS$ and $CeAg_{0.8}OS$, the closest S···S distances are 3.907 and 3.923 Å, respectively, so there is no S−S bonding. With formal oxidation states of 2−, 2−, and 1+ for O, S, and Ag, respectively, the Ce atoms in $CeAg_{0.8}OS$ must comprise 20% Ce^{4+} and 80% Ce^{3+}. Because the 2+ oxidation state is more accessible in Cu than in Ag, the oxidation states of Cu and Ce in $CeCu_{0.8}OS$ are not as easy to assign. Nevertheless, the existence of the Ag analogue strongly suggests Cu^{1+} and 20% Ce^{4+} and 80% Ce^{3+} in $CeCu_{0.8}OS$. Soft bond valence[30,31] calculations are frequently invoked to provide a guide to the distribution of oxidation states in a given crystal structure. In the present instance, such calculations were performed for the crystal structures of LnCuOS (Ln = La, Pr, and Nd), as well as for $CeCu_{0.809(4)}OS$ and $CeCu_{0.762(4)}OS$. With the caveat that the method is strictly empirical, the results presented in Table 3 suggest that the formal oxidation state of Ce in the present compounds and in the CeCuOS powder sample prepared earlier[12] is perhaps higher than are the oxidation states of Ln in the others compounds. The latter are presumed to be 3.0. The formal oxidation states of Cu are underestimated for all Ln. However, their consistency suggests that all the compounds contain Cu^{1+}, as is expected for stoichiometric LnCuOS (Ln other than Ce). Hence, the results in Table 3 are consistent with the existence of mixed-valence Ce^{4+}/Ce^{3+} in $CeCu_{0.8}OS$ and they point to possible Cu deficiencies in the powder sample of CeCuOS.[12]

Magnetic Susceptibility. The molar magnetic susceptibilities, χ_m, as well as χ_m^{-1}, of single crystals of $CeCu_{0.8}OS$ and a powder sample of CeAgOS as a function of temperature are shown in Figure 3. There is no apparent magnetic ordering down to 5 K. Both compounds are paramagnetic, showing Curie−Weiss behavior $\chi_m^{-1} = (T - \theta_p)/C$, in the temperature region between 100 and 350 K. However, below

(24) Johnson, V.; Jeitschko, W. *J. Solid State Chem.* **1974**, *11*, 161−166.
(25) Céolin, R.; Rodier, N. *Acta Crystallogr.* **1976**, *B32*, 1476−1479.
(26) Huang, F. Q.; Brazis, P.; Kannewurf, C. R.; Ibers, J. A. *J. Solid State Chem.* **2000**, *155*, 366−371.
(27) Ijjaali, I.; Haynes, C. L.; McFarland, A. D.; Van Duyne, R. P.; Ibers, J. A. *J. Solid State Chem.* **2003**, *172*, 257−260.
(28) Pervukhina, N. V.; Atuchin, V. V.; Parasyuk, O. V. *Acta Crystallogr. Sect. E: Struct. Rep. Online* **2005**, *e61*, i91−i93.
(29) Emirdag, M.; Schimek, G. L.; Kolis, J. W. *Acta Crystallogr. Sect. C: Cryst. Struct. Commun.* **1998**, *54*, 1376−1378.
(30) Brown, I. D.; Altermatt, D. *Acta Crystallogr. Sect. B: Struct. Sci.* **1985**, *41*, 244−247.
(31) Adams, S. *Acta Crystallogr. Sect. B: Struct. Sci.* **2001**, *57*, 278−287.

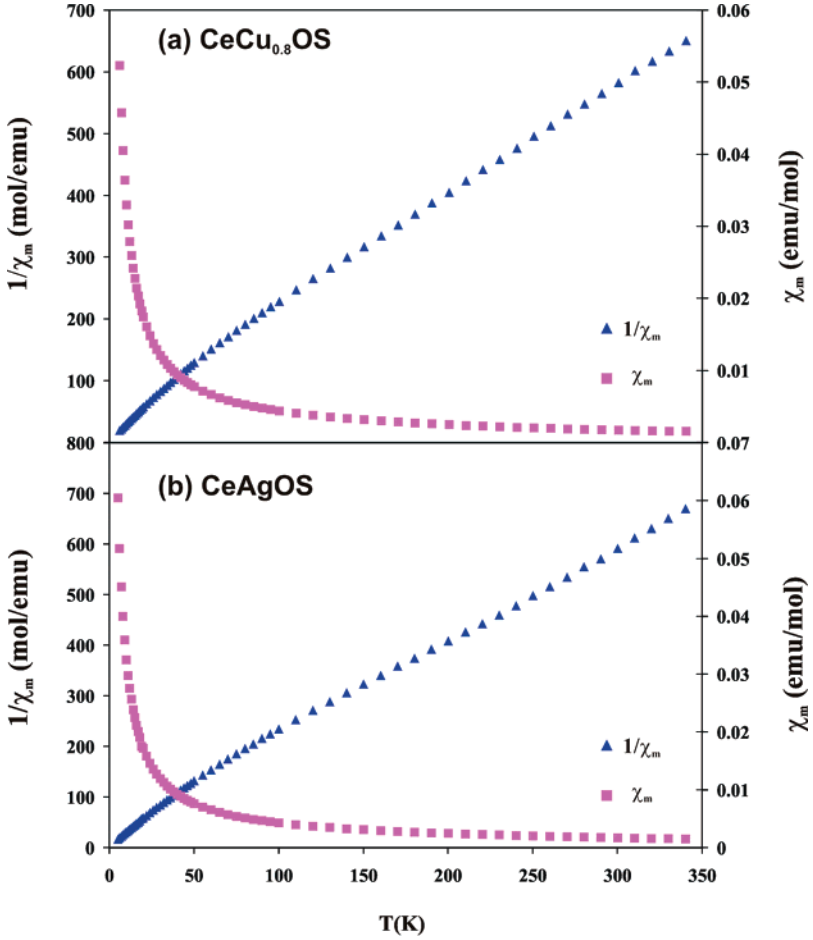

Figure 3. Molar magnetic susceptibility, χ_m, and inverse molar magnetic susceptibility, χ_m^{-1}, vs T for ZFC data. (a) Ground single crystals of $CeCu_{0.8}OS$, (b) CeAgOS powder. FC data (not shown) are very similar.

80 K, there is deviation from Curie−Weiss behavior as a result of the crystal-field splitting in the $J = 5/2$ ground states of the Ce^{3+} ($4f^15s^2p^6$) cations. Of course, the LaMOS (M = Cu, Ag) compounds are diamagnetic.

The values of the Curie constant, C, the Weiss constant, θ_p, and the effective magnetic moment, μ_{eff}, are 0.569(2) emu·K/mol, −30.2(1) K, and 2.13(6) μ_B, respectively, for $CeCu_{0.8}OS$ and 0.554(5) emu·K/mol, −28.1(3) K, and 2.10(1) μ_B, respectively, for CeAgOS. From the theoretical Curie constants[32] (Ce^{3+}, 0.806; Cu^{2+}, 0.315 (L−S coupling) or 0.374 emu·K/mol (spin only)), theoretical values of 2.27 μ_B for $Ce^{4+}{}_{0.2}Ce^{3+}{}_{0.8}Cu^{1+}{}_{0.8}OS$ and 2.64 μ_B (L−S) or 2.65 μ_B (spin only) for $Ce^{3+}Cu^{2+}{}_{0.2}Cu^{1+}{}_{0.6}OS$ are calculated. The experimental effective magnetic moments of both compounds confirm the presence of Ce^{3+}. However, because the high concentration of diamagnetic species most likely dominates any Pauli paramagnetic signal, the magnetic data cannot be used to confirm the presence of Cu^{2+} as a minor component. Note that a value of $\mu_{eff} = 2.1$ μ_B was also reported earlier for CeCuOS.[12]

Transport Properties. The electrical conductivity, σ, measured along the *ab* plane of a single crystal of $CeCu_{0.8}OS$ is shown as a function of inverse temperaturein Figure 4. The material is a semiconductor with σ increasing with T; σ is 9.8(1) 10^{-3} S/cm at 298 K. Hall effect measurements indicate the hole carrier concentration is approximately 3×10^{16} with a mobility of 1.5 $cm^2/V{\cdot}s$. An Arrhenius fit to the data leads to a thermal activation energy E_a of 0.22 eV. A value of σ of 6.1×10^{-1} S/cm at 298 K was reported for a sintered disk of CeCuOS.[8] This discrepancy in electrical conductivity may result from differences in preparation of the samples (single crystal vs sintered disk), as well as the number of Cu vacancies in our samples. Electronic structure calculations indicate that the hole carriers of LnCuOS (Ln

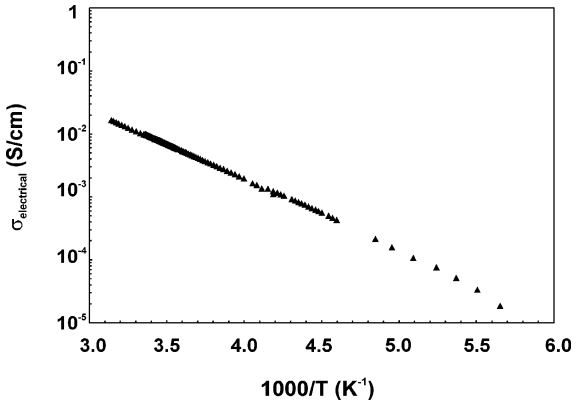

Figure 4. Single-crystal electrical conductivity σ along the *ab* plane vs T^{-1} for $CeCu_{0.8}OS$.

(32) Kittel, C. *Introduction to Solid State Physics*, 7th ed.; Wiley: New York, 1996.

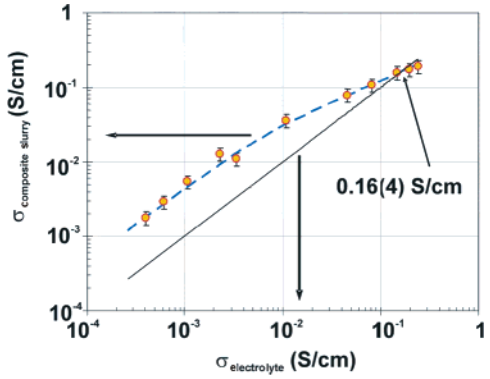

Figure 5. Total PSC-derived conductivity[20] of CeAgOS salt solution composites vs the conductivity of the NaCl electrolyte. The solid line is the conductivity of the electrolyte, and the dashed curve represents the theoretical fit (see text) through the experimental data. The crossover point shows the approximate CeAgOS particle conductivity, with error bars as shown.

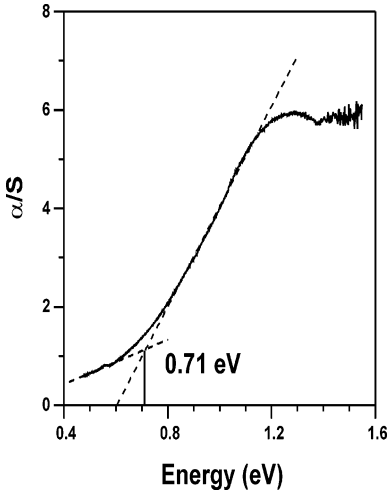

Figure 6. Diffuse reflectance spectrum of CeAgOS.

= La, Ce, Pr, and Nd) originate from the $(Cu_2S_2)^{2-}$ layer. If Cu vacancies are introduced into the $(Cu_2S_2)^{2-}$ layer, then σ should be lowered. The present value of σ of 9.8(1) 10^{-3} S/cm for $CeCu_{0.8}OS$ is still larger than the values of 8.0×10^{-6}, 1.6×10^{-5}, and 3.8×10^{-4} S/cm found for sintered disks of LaCuOS, PrCuOS, and NdCuOS, respectively.[8]

The conductivity of CeAgOS powder was measured by the PSC technique,[20] which does not distinguish between ionic and electrical conductivity. The PSC plot is shown in Figure 5. The value of σ of 0.16(4) S/cm at 298 K is deduced from the intersection of the conductivity lines of the NaCl electrolyte solution and the composite NaCl/CeAgOS slurry. Some known compounds that contain both Ag and Q elements, such as Ag_2Q (Q = S, Se)[33] and $Ag_4Hf_3S_8$,[34] tend to display both electrical conductivity and ionic conductivity. For LaAgOS, activation energies of 0.22 eV[7] and 0.195 eV[4,5] have been reported, as well as values of $\sigma_{ionic} = 10^{-3}-10^{-1}$ S/cm between 298 and 523 K.[5] Because CeAgOS is isostructural to LaAgOS, it is very probable that CeAgOS is also an ionic conductor. Note, in particular, that the principal mean-square displacements of Ag in the $CeAg_{0.8}OS$ crystal structure markedly increase from 0.0246, 0.0226, and 0.0062 Å^2 at 153 K to 0.0792, 0.0611, and 0.0087 Å^2 at 298 K. Large displacements for Ag were also seen in the structure of LaAgOS at 298 K.

Optical Band Gaps. Optical measurements[1] (400−1700 nm) were performed on a single crystal of $CeCu_{0.8}OS$, but no visible absorption edge was detected. This suggests that the optical band gap of $CeCu_{0.8}OS$ is less than 0.73 eV but greater than the thermal activation energy of 0.22 eV, consistent with its black color and a calculated band gap of 0.6 eV (see below). The diffuse reflectance spectrum of CeAgOS powder is depicted in Figure 6. The derived value of 0.71 eV is consistent with the black color of the compound. LaAgOS is green; hence the substitution of Ce for La in LnAgOS decreases the optical band gap.

Electronic Structure. $CeCu_{0.8}OS$ and $CeAg_xOS$ ($x = 0.8$, 1.0) are black, distinctly different in color from those of the LnMOS (Ln = La, Pr, and Nd; M = Cu, Ag) compounds. In first-principles calculations, the Ln 4f states are generally treated as part of the core states; therefore, the Ln 4f states do not contribute at the Fermi level, and such calculations do not differentiate among various Ln. Recently, a Hubbard on-site Coulomb repulsion parameter, U, has been introduced into such calculations—LDA+U or GGA+U.[22,23] A large value of U (>10.0 eV) has generally been used to account for the highly localized Ln 4f states found for most Ln metals except for Ce whose 4f electrons tend to be less localized. The most recent calculated U parameters for Ce from GGA+U using the linear response approach have been determined to be 1.5−2 eV.[35] Therefore, in our calculations the value of U of 2.0 eV was used. As a reminder, the electronic structure calculations of $CeCu_{0.75}OS$ represent those of $CeCu_{0.8}OS$.

The total and partial density of states (DOS) of CeCuOS, CeAgOS, and $CeCu_{0.75}OS$ are similar. The total and partial DOS of $CeCu_{0.75}OS$ are shown in Figure 7. Diagrams of the total and partial DOS of CeCuOS and CeAgOS may be found in the Supporting Information. The Ce 4f states are mainly located around the Fermi level in both the valence and conduction bands. These states show up in the DOS of the majority spin (spin up), but not in the DOS of the minority spin (spin down). Thus, the Ce 4f states are mostly fully polarized. Antibonding states of Cu 3d (or Ag 4d) and S 3p are located in the top part of the valence band. O 2p states and Ce 5d states are mainly located in the region from −6 to −2 eV, where they are highly hybridized. There is minimal contribution from either the O 2s or the O 2p states in the valence band near the Fermi level, which suggests that Ce 4f states do not mix with either the valence or the conduction bands.

The energy-band diagrams for majority and minority spin of $CeCu_{0.75}OS$ are shown in Figure 8. Energy-band diagrams for majority and minority spin of CeAgOS and CeCuOS may be found in the Supporting Information. The band diagrams for minority spin of CeCuOS, CeAgOS, and $CeCu_{0.75}OS$ are

(33) Kashida, S.; Watanabe, N.; Hasegawa, T.; Iida, H.; Mori, M.; Savrasov, S. *Solid State Ionics* **2003**, *158*, 167−175.
(34) Amiel, O.; Wada, H. *J. Solid State Chem.* **1995**, *115*, 112−119.
(35) Fabris, S.; de Gironcoli, S.; Baroni, S.; Vicario, G.; Balducci, G. *Phys. Rev. B* **2005**, *71*, 041102−1−041102−4.

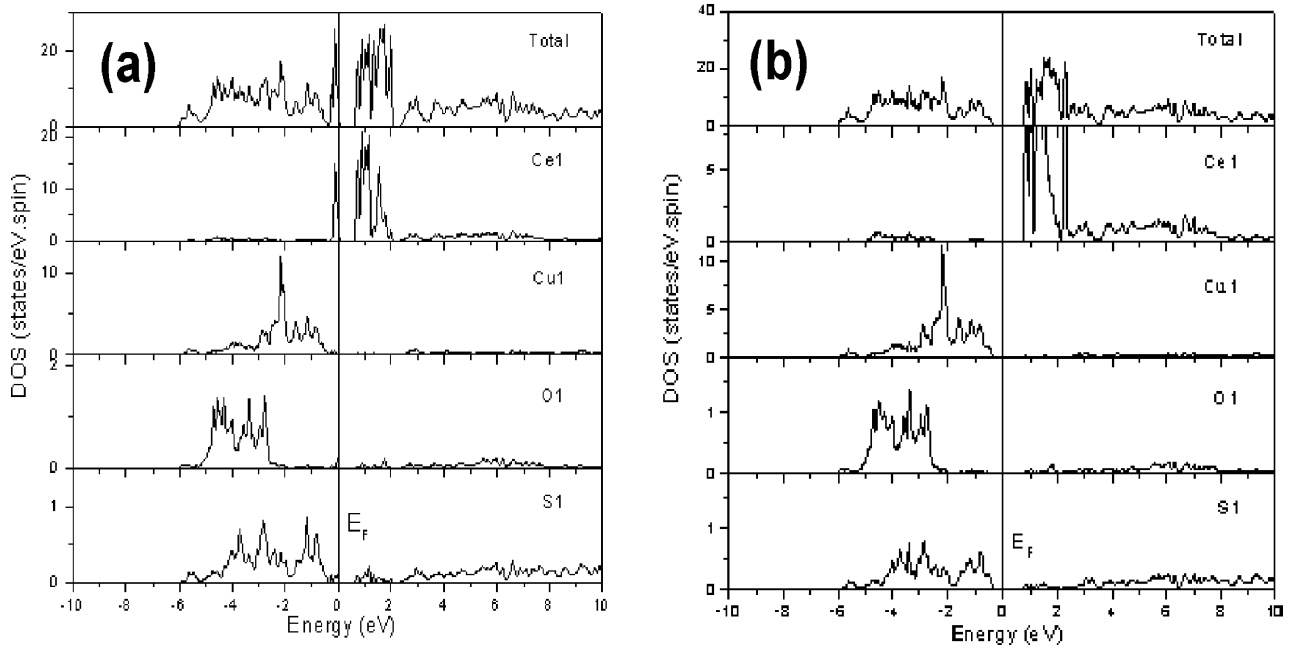

Figure 7. Total and partial DOS of $CeCu_{0.75}OS$ (hence $CeCu_{0.8}OS$) for (a) majority spin and (b) minority spin. In each case, the partial DOS is shown for one unique atom in the 2×1 supercell used for the calculations. Differences among unique atoms are minimal.

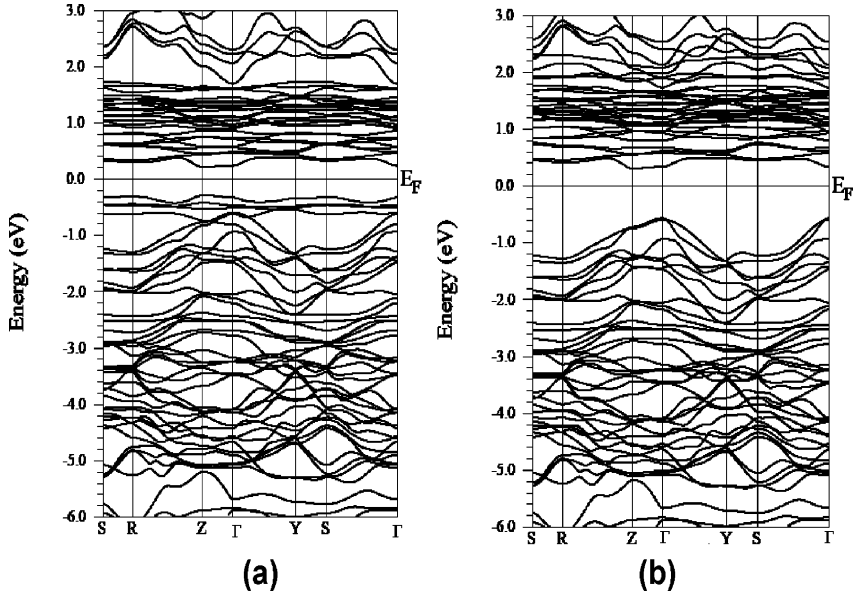

Figure 8. Energy-band structure of $CeCu_{0.75}OS$ (hence $CeCu_{0.8}OS$) for (a) majority spin and (b) minority spin. Special points are *S* (−1/2,1/2,0), *R* (−1/2,1/2,1/2), *Z* (0,0,1/2), Γ (0,0,0), and *Y* (−1/2,0,0).

similar, but those for majority spin show differences. The latter were used to derive band gaps. As deduced from the band diagrams, the band gap in $CeCu_{0.75}OS$ is smaller than that in stoichiometric CeCuOS. Thus, in stoichiometric CeCuOS (majority spin), the minimum band gap is not located at the Γ point but rather at the *M* point with the value of about 1.5 eV assigned as an indirect transition. In nonstoichiometric $CeCu_{0.75}OS$ (majority spin), the calculated direct band gap is about 0.6 eV at the *Z* point, a value consistent with experimental data, as well as with the black color of $CeCu_{0.8}OS$. In CeAgOS (majority spin), the conduction band minimum is located at the Γ point, whereas the valence band maximum is located at the *M* point. The indirect band gap between *M* and Γ is nearly zero. Moreover, transitions from different symmetries may be weak or forbidden. Hence, we assign a direct band gap at the Γ point of 0.8 eV to CeAgOS, in close agreement with the experimental value of 0.71 eV. This agreement may be fortuitous because calculated band gaps are very sensitive to the chosen value of *U*. For example, the calculated band gap of CeAgOS is about 2.1 eV for a *U* of 4.5 eV, whereas for a *U* less than 1.0 eV, the Ce 4f states cannot be removed from the Fermi level. The resultant metallic ground state is inconsistent with our experimental results. For comparison, we have also calculated the band diagram and the total and partial DOS of LaAgOS (Supporting Information). LaAgOS is determined to have a direct band gap of about 1.2 eV, larger than that of CeAgOS, as expected from the colors of these compounds. The band-

Table 4. Unit Cell Parameters for LnMOS Compounds[a]

compound	a (Å)	c (Å)	V (Å^3)	ref
LaCuOS	3.999(1)	8.53(1)	136.5(5)	3
LaCuOS	3.99625(4)	8.51743(9)	136.023(2)	12
$CeCu_{1-x}OS$[b]	3.919(1)	8.432(3)	129.5(1)	11
$CeCu_{0.95}OS$	3.917(2)	8.412(3)	129.0(1)	11
$CeCu_{0.90}OS$	3.918(1)	8.394(5)	128.8(2)	11
$CeCu_{0.85}OS$	3.911(1)	8.365(3)	127.9(1)	11
CeCuOS	3.9228(1)	8.3475(3)	128.46(1)	12
$CeCu_{0.762(4)}OS$ (298 K)[c]	3.9072(3)	8.2834(10)	126.46(2)	this work
$CeCu_{0.809(4)}OS$ (153 K)[c]	3.9142(3)	8.2980(10)	127.13(2)	this work
PrCuOS	3.939(1)	8.438(3)	130.9(1)	11
	3.9419(4)	8.4398(9)	131.14(6)	39[c]
	3.94148(9)	8.4376(1)	131.081(5)	12
NdCuOS	3.918(1)	8.434(6)	129.5(2)	11
	3.903(5)	8.480(1)	129.1(8)	36
	3.9196(1)	8.4282(2)	129.487(6)	12
SmCuOS	3.887(3)	8.385(7)	126.7(3)	11
	3.854(3)	8.442(7)	125.3(9)	36
EuCuOS	3.874(2)	8.379(6)	125.8(2)	11

[a] X-ray powder data, unless otherwise noted. [b] Sample was in equilibrium with excess Cu.[11] [c] Single-crystal X-ray data.

width of CeAgOS (1.2 eV) is similar to that of LaAgOS. This indicates that the hybridization between the Ag 4d and S 3p states is similar. The bandwidth of CeCuOS (1.0 eV) indicates that the hybridization of the Cu 3d and S 3p states is weaker than that of the Ag 4d and S 3p states in CeAgOS. Because of the Cu deficiencies, the Cu 3d and S 3p interactions in $CeCu_{0.75}OS$ are weakened and the bandwidth is much smaller, about 0.6 eV.

Anomalous Shrinkage. Table 4 lists the unit-cell parameters known for LnCuOS compounds (Ln = La, Ce, Pr, Nd, Sm, and Eu). Generally, there is minimal information on the materials and techniques employed to arrive at these unit-cell parameters. Because of uncertainties involving compound composition and pattern calibration, the following discussion is qualitative. That CeCuOS does not follow the expected lanthanide contraction of the unit-cell volume has been noted[11,12] and is apparent in Figure 1 and Table 4. Given the structure of the LnCuOS compounds, one would anticipate that the effect of the lanthanide contraction should be greatest in the c direction, which is perpendicular to the layers. This is also apparent in Table 4. The volume $V = a^2c$ de-emphasizes the effect of the lanthanide contraction and the anomalous nature of CeCuOS.

Within the $CeCu_xOS$ series, the c lattice constant decreases as x decreases. This also follows from the crystal structure. This effect holds even for the two entries from the present study: the presumed temperature contraction of the c lattice constant is smaller than the increase in that lattice constant with composition. The results for the stated composition CeCuOS[12] are anomalous but would not be if x were approximately 0.83, rather than 1.0 as claimed. The presence of Cu vacancies in this compound is consistent with the large anisotropic displacement parameters for Cu found in its structure.[12] From our crystal structures, chemical analysis, and failure to synthesize a single crystal of composition $CeCu_{1.0}OS$, we believe that the formation of Cu vacancies is intrinsic to this compound and that nonstoichiometry and hence the presence of Ce^{4+} explains the anomaly seen in Table 4.

Can we estimate the maximum number of Cu vacancies in the $CeCu_xOS$ series before the structure is unstable? A geometrical structural study[36] proposed that the termination of the series LnCuOS at Ln = Sm is the result of reaching the limiting Cu−Cu distance of 2.72 Å where the distortion of Cu tetrahedra can no longer sustain the change in the size of the lanthanide ion. If we consider the ionic radii[37] for eight-coordinate $Ce^{3+}$and Ce^{4+} of 1.143 and 0.97 Å, and set the average Ce radius in $Ce^{3+}{}_{1-x}Ce^{4+}{}_xCu^{1+}{}_{1-x}OS$ equal to that of Sm^{3+} (1.079 Å), then $x = 0.37$. This suggests that instability would set in at about the composition $Ce^{3+}{}_{0.6}Ce^{4+}{}_{0.4}Cu_{0.6}OS$.

Acknowledgment. We acknowledge Dr. Stephan Adams, Dr. Byron Watkins, and Dr. Hiroshi Mizoguchi for their helpful comments. We thank Ms. Jill Millstone and Dr. Chad A. Mirkin for help with the use of their UV−vis spectrometer and Mr. Jiha Sung and Dr. Kenneth G. Spears for the use of their NIR spectrometer. We are also grateful to Ms. Danielle Gray for her help with ICP measurements. This research was supported in part by National Science Foundation Grant No. DMR00-96676 and Department of Energy BES Grant ER-15522 and a Northwestern University MRSEC Fellowship (G.H.C.). Use was made of the Central Facilities supported by the MRSEC program of the National Science Foundation (DMR00-76097) at the Materials Research Center of Northwestern University.

Supporting Information Available: Crystallographic files in CIF format for CeM_xOS (M = Cu, Ag) at 153 and 298 K; the total and partial DOS and energy-band structures of majority spin and minority spin CeCuOS and CeAgOS; and the total and partial DOS of LaAgOS. This material is available free of charge via the Internet at http://pubs.acs.org.

IC061041K

(36) Popovkin, B. A.; Kusainova, A. M.; Dolgikh, V. A.; Aksel'rud, L. G. *Russ. J. Inorg. Chem. (Transl. of Zh. Neorg. Khim.)* **1998**, *43*, 1471−1475.
(37) Shannon, R. D. *Acta Crystallogr. Sect. A: Cryst. Phys. Diffr. Theor. Gen. Crystallogr.* **1976**, *32*, 751−767.
(38) Wu, L. B.; Liu, M. L.; Huang, F. Q.; Chen, L. D.; Ibers, J. A. *J. Solid State Chem.* **2006**, submitted for publication.
(39) Lauxmann, P.; Schleid, T. *Z. Anorg. Allg. Chem.* **2000**, *626*, 2253−2255.
(40) Kusainova, A. M.; Berdonosov, P. S.; Akselrud, L. G.; Kholodkovskaya, L. N.; Dolgikh, V. A.; Popovkin, B. A. *J. Solid State Chem.* **1994**, *112*, 189−191.